BIOCHEMISTRY
including biophysical chemistry & molecular biology

Article

pubs.acs.org/biochemistry

Structural and Kinetic Studies on Metallo-β-lactamase IMP-1

Dionne H. Griffin,[†] Timothy K. Richmond,[†] Carlo Sanchez,[†] Abraham Jon Moller,[†] Robert M. Breece,[†] David L. Tierney,[†] Brian Bennett,[‡] and Michael W. Crowder*[,†]

[†]Department of Chemistry and Biochemistry, 160 Hughes Hall, Miami University, Oxford, Ohio 45056, United States

[‡]National Biomedical EPR Center, Department of Biophysics, Medical College of Wisconsin, Milwaukee, Wisconsin 53226, United States

Supporting Information

ABSTRACT: In an effort to probe for metal binding to metallo-β-lactamase (MβL) IMP-1, the enzyme was overexpressed, purified, and characterized. The resulting enzyme was shown to bind 2 equiv of Zn(II), exhibit significant catalytic activity, and yield EXAFS results similar to crystallographic data previously reported. Rapid kinetic studies showed that IMP-1 does not stabilize a nitrocefin-derived reaction intermediate; rather, the enzyme follows a simple Michaelis mechanism to hydrolyze nitrocefin. Metal-substituted and metal-reconstituted analogues of IMP-1 were prepared by directly adding metal ion stocks to metal-free enzyme, which was generated by dialysis versus EDTA. UV−vis studies on IMP-1 containing 1 equiv of Co(II) showed a strong ligand-to-metal charge transition at 340 nm, and the intensity of this feature increased when the second equivalent of Co(II) was added to the enzyme. EXAFS fits on IMP-1 containing 1 equiv of Co(II) strongly suggest the presence of a metal−metal interaction, and EPR spectra of the IMP-1 containing 1 and 2 equiv of Co(II) are very similar. Taken together, steady-state kinetic and spectroscopic studies suggest that metal binding to metal-free IMP-1 follows a positive-cooperative mode.

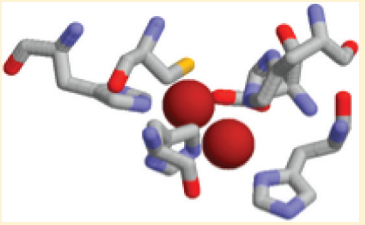

Due to the misuse of carbapenems and extended-spectrum cephalosporins, acquired metallo-β-lactamases (MβLs) are emerging in Gram-negative pathogens, including *Acinetobacter spp.* and *Pseudomonas aeruginosa*.[1−3] A large number of acquired MβLs have been identified during the past few years, including IMP-1, VIM-1, GIM-1, SPM-1, NDM-1, and SIM-1.[1,4] The spread of resistance is not merely shared among species but extends into different genera via horizontal gene transfer. This scenario is exemplified by metallo-β-lactamase IMP-1, which was initially isolated in the early 1990s from *Pseudomonas aeruginosa* and *Serratia marcescens*.[5,6] Since this time, the bla_{IMP-1} gene has also been detected in isolates of *Klebsiella pneumoniae, Pseudomonas putida, Alcaligenes xylosoxidans, Acinetobacter junii, Providencia rettgeri, Acinetobacter baumannii, and Enterobacter aerogenes*.[1] Many of the plasmids containing the bla_{IMP-1} gene also encode for additional antibiotic resistance mechanisms, i.e., aminoglycosidase.[7] Because of the ability of the bla_{IMP} gene to spread rapidly by horizontal transfer, isolates have been identified in South East Asia, Europe, and the Americas.[3,8]

To date, 27 variants of IMP-1 have been isolated from around the world.[8] Biochemical characterization of these variants has revealed structural and functional differences. Three minor variants of IMP-1 have been identified and called IMP-3,[9] IMP-6,[10] and IMP-10.[11] The most divergent is IMP-12 possessing 36 different amino acids.[12] The IMP enzymes exhibit broad substrate specificity, with high affinities for cephalosporins and carbapenems rather than for penicillins.[1,8] By far, the best studied variant is IMP-1, which belongs to the B1 subclass of MβLs.[13] Crystal structures of IMP-1 show an αβ/αβ sandwich fold, wherein the catalytic dinuclear zinc-binding site lies at the interface of the two αβ domains.[14−16] One Zn(II) (Zn_1 site) is coordinated by His116, His119, His196, and a bridging water/hydroxide, while the second Zn(II) (Zn_2 site) is bound by Asp120, Cys221, His263, a terminally bound water, and the bridging solvent molecule. The Zn(II)−Zn(II) distance is 3.5−3.7 Å.

Several of the MβLs (Zn(II)-containing and Co(II)-substituted forms) have been extensively studied using various spectroscopic techniques, such as ^{1}H NMR, UV−vis, EPR, and EXAFS spectroscopies.[17−23] However, the number of spectroscopic studies on IMP-1 or any of the IMP variants is relatively small. Metallo-β-lactamase IMP-1 is considered to be one of the most clinically important MβLs for several reasons: (i) most IMP variants hydrolyze all β-lactam containing antibiotics, except monobactams, including carbapenems like imipenem; (ii) the gene for IMP, bla_{IMP-1} has rapidly spread in many pathogenic bacteria; and (iii) IMP has mutated to at least 27 different variants, each exhibiting different hydrolysis rates, stabilities, etc. This paper describes our efforts at preparing and characterizing Co(II)-substituted IMP-1. These studies will allow for the future use of rapid-freeze quench spectroscopic studies to probe the active site structures and mechanisms of IMP-1 and the IMP variants.

EXPERIMENTAL PROCEDURES

Materials. The *pet26b-IMP-1* plasmid (originally isolated from clinical strain of *Serratia marcescens* producing IMP-1) was

Received: May 31, 2011
Revised: September 16, 2011
Published: September 19, 2011

a gift from Dr. James Spencer (Department of Cellular and Molecular Medicine, University of Bristol, School of Medical Sciences, University Walk, Bristol BS8 1TD, U.K.). *E. coli* BL21(DE3) was used for the overexpression of IMP-1 via the T7 expression system (Novagen Inc., Madison, WI). IMP-1 was overexpressed in Luria−Bertani medium (LB) purchased from Invitrogen (Carlsbad, CA) or in minimum medium, as previously reported.[20] Isopropyl β-D-thiogalactoside (IPTG) was purchased from Anatrace (Maumee, OH). Recombinant IMP-1 was purified on a SP-Sepharose column (GE Healthcare). Purified protein solutions were concentrated with an Amicon ultrafiltration cell equipped with YM-10 DIAFLO membranes from Amicon, Inc. (Beverly, MA). Kinetic studies were conducted using nitrocefin purchased from Becton Dickinson (Franklin Lakes, NJ).[24]

Overexpression and Purification of IMP-1 in Rich Medium. To obtain large quantities of IMP-1, a 50 mL preculture of *E. coli* BL21(DE3) harboring the *pet26b-IMP-1* plasmid was used to inoculate 4 × 1 L of Luria−Bertani (LB) medium. Kanamycin (25 μg/mL) was used as a selection agent during overexpression. The innoculum was grown at 37 °C until the culture reached an optical density ($OD_{600\,nm}$) of 0.8−1.0. Protein production was induced by making the cultures 0.5 mM in isopropyl-β-D-thiogalactopyranoside (IPTG). The cultures were further incubated overnight at 22 °C for ∼20 h. Cells were collected by centrifugation (8000*g*) for 10 min. The resulting pellet was resuspended in 25 mL of 50 mM 4-(2-hydroxymethyl)-1-piperazineethanesulfonic acid (HEPES), pH 7.5 (buffer A). The cells were lysed by passing the resuspended cells through a French Press three times at a pressures between 3.5 and 7.0 MPa. The lysate was clarified by centrifugation at 15000*g* for 30 min. The supernatant was dialyzed versus 1 L of 50 mM HEPES, pH 7.5, overnight at 4 °C. To remove precipated protein and other insoluble components, the dialyzed sample was centrifuged for 30 min at 15000*g*. The sample solution was loaded onto an SP-Sepharose column (1.5 × 12 cm with a 25 mL bed volume), which was pre-equilibrated in 50 mM HEPES, pH 7.5. Bound proteins were eluted with 0−500 mM NaCl gradient in 50 mM HEPES, pH 7.5 (buffer B). Purity of the fractions was ascertained by SDS-PAGE gels. Those fractions containing pure IMP-1 were pooled and concentrated by using an Amicon ultrafiltration concentrator equipped with a YM-10 membrane. IMP-1 concentrations were determined using the extinction coefficient ($\varepsilon_{280\,nm}$ = 49 000 M^{-1} cm^{-1}), as reported by Yamaguchi et al.[16] The extinction coefficient for all Zn(II)- and Co(II)-containing analogues of IMP-1 and for apo-IMP-1 was also found to be 49 000 M^{-1} cm^{-1}.

Metal Analyses. Inductively coupled plasma atomic emission spectroscopy (ICP-AES) was used to determine the metal content of IMP-1 samples. Purified enzyme samples were diluted to ∼10 μM in 50 mM HEPES, pH 6.8 or 7.5. Calibration curves exhibiting correlation coefficients of greater than 0.9999 were generated using serial dilutions of Fisher metal standards (Zn, Co, Cu, Fe, Mn, and Ni) ranging from 3.0 to 35 μM. Emission lines at 213.856, 238.892, 324.754, 259.940, 257.610, and 231.604 nm were chosen to ensure the lowest possible detection limits for zinc, cobalt, copper, iron, manganese, and nickel, respectively.

Steady-State Kinetics. Steady-state kinetic studies were conducted on a Hewlett-Packard 5480A UV−vis spectrophotometer at 25 °C. The hydrolysis of nitrocefin by IMP-1 was monitored by following the formation of the hydrolyzed product at 485 nm. The molar absorptivity of nitrocefin ($\Delta\varepsilon_{485\,nm}$ = 17 400 M^{-1} cm^{-1})[25] was used to determine the rates of hydrolysis. Substrate concentrations ranged from 10 to 200 μM or until significant substrate inhibition was observed. The enzyme concentration in the reactions was ca. 3 nM. All reactions were performed in 50 mM HEPES, pH 6.8 or 7.5, with total volume of 1 mL.

Stopped-Flow Kinetic Studies. To probe the reaction mechanism, stopped-flow UV−vis studies were conducted on an Applied Photophysics SX.18-MVR stopped-flow spectrophotometer at 4 °C. UV−vis spectra were recorded from 300 to 700 nm. Near single-turnover reactions were conducted with the use of 1:1 ratio of IMP-1:nitrocefin. Progress curves (absorbance change over time) from stopped-flow studies were converted to concentration of nitrocefin or concentration of hydrolyzed nitrocefin versus time by using the molar extinction coefficients of nitrocefin and hydrolyzed nitrocefin, respectively. Experiments were conducted in triplicate, and the data from the experiments were averaged. Simulated progress curves were generated by using a MATLAB script derived for three possible mechanisms (Scheme 1). The theoretical k_{cat} and K_m expressions for each mechanism were derived using the King−Altman method,[26] assuming k_2 (or k_3 in (2)) as the rate-limiting step. Rate constants were varied to fit the simulated curves to experimental presteady state data and to calculated "theoretical" k_{cat} and K_m values that matched experimental values. The rate constants for the binding of substrate and product (k_1 and k_{-3} or k_{-4} for (2)) were set to the diffusion-limited value of 10^8 M^{-1} s^{-1}.

Scheme 1

$$(1)\quad \mathbf{E} + \mathbf{S} \underset{k_{-1}}{\overset{k_1}{\rightleftharpoons}} \mathbf{ES} \underset{k_{-2}}{\overset{k_2}{\rightleftharpoons}} \mathbf{EP} \underset{k_{-3}}{\overset{k_3}{\rightleftharpoons}} \mathbf{E} + \mathbf{P}$$

$$(2)\quad \mathbf{E} + \mathbf{S} \underset{k_{-1}}{\overset{k_1}{\rightleftharpoons}} \mathbf{ES} \underset{k_{-2}}{\overset{k_2}{\rightleftharpoons}} \mathbf{EI} \underset{k_{-3}}{\overset{k_3}{\rightleftharpoons}} \mathbf{EP} \underset{k_{-4}}{\overset{k_4}{\rightleftharpoons}} \mathbf{E} + \mathbf{P}$$

$$(3)\quad \mathbf{E} + \mathbf{S} \underset{k_{-1}}{\overset{k_1}{\rightleftharpoons}} \mathbf{ES} \underset{k_{-2}}{\overset{k_2}{\rightleftharpoons}} \mathbf{ES^*} \underset{k_{-3}}{\overset{k_3}{\rightleftharpoons}} \mathbf{E} + \mathbf{P}$$

EXAFS Spectroscopy. Samples of IMP-1 with 1 or 2 added equivalents of Zn(II) or Co(II) (0.8−1.5 mM) were prepared containing ca. 30% (v/v) glycerol as glassing agent, loaded into Lucite cuvettes with 6 μm polypropylene windows, and flash frozen in liquid nitrogen. X-ray absorption spectra were measured at the National Synchrotron Light Source (NSLS), beamline X3B, using a Si(111) double crystal monochromator; harmonic rejection was accomplished using a Ni focusing mirror. Fluorescence excitation spectra were measured with a 13-element solid-state Ge array detector. Samples were held at ∼15 K in a Displex cryostat during XAS measurements. X-ray energies were calibrated by reference to the absorption spectrum of the appropriate metal foil, measured concurrently with the protein spectra. All of the data shown represent the average of ∼12 total scans, from two independently prepared samples for each stoichiometry. Data collection and reduction were performed according to published procedures[21,27] with E_0 set to 9675 eV for Zn and 7730 eV for Co. The Fourier-filtered EXAFS were fitted

to eq 1 using the nonlinear least-squares engine of IFEFFIT that is distributed with SixPack[28] Sixpack is available free of charge from http://www-sssrl.slac.stanford.edu/~swebb/index.htm.

$$\chi(k) = \sum \frac{N_{as}A_s(k)S_c}{kR_{as}^2} \exp(-2k^2\sigma_{as}^2) \exp(-2R_{as}/\lambda) \sin[2kR_{as} + \phi_{as}(k)] \quad (1)$$

In eq 1, N_{as} is the number of scattering atoms within a given radius (R_{as}, $\pm\sigma_{as}$), $A_s(k)$ is the backscattering amplitude of the absorber−scatterer (as) pair, S_c is a scale factor, $\phi_{as}(k)$ is the phase shift experienced by the photoelectron, λ is the photoelectron mean free path, and the sum is taken over all shells of scattering atoms included in the fit. Theoretical amplitude and phase functions, $A_s(k)\exp(-2R_{as}/\lambda)$ and $\phi_{as}(k)$, were calculated using FEFF v. 8.00.[29] The scale factor (S_c) and ΔE_0 for Zn−N (S_c = 0.78, ΔE_0 = −16 eV), Zn−S (0.85, −16 eV), Co−N (0.74, −21 eV), and Co−S (0.85, −21 eV) scattering were determined previously and held fixed throughout this analysis.[21,27] Fits to the current data were obtained for all reasonable integer or half-integer coordination numbers, refining only R_{as} and σ_{as}^2 for a given shell. Multiple scattering (ms) contributions from histidine ligands were approximated according to published procedures,[21,27] fixing the number of imidazole ligands per metal ion at half-integral values while varying R_{as} and σ_{as}^2 for each of the four combined ms pathways. Metal−metal (Co−Co and Zn−Zn) scattering was modeled by fitting calculated amplitude and phase functions to the experimental EXAFS of $Co_2(salpn)_2$ and $Zn_2(salpn)_2$.

Preparation of Metal-Free IMP-1. Recombinant IMP-1 was overexpressed and purified as described above. A dilute solution of IMP-1 (ca. 20−30 μM) was dialyzed against 4 × 1 L (12 h per step) of 50 mM HEPES, pH 6.8, containing 10 mM 1,10-phenanthroline or 10 mM EDTA, at 4 °C. The chelating agent was removed by dialysis against 6 × 1 L of Chelex-treated, 50 mM HEPES, pH 6.8, containing 0.5 M NaCl. ICP-AES mea surements were used to determine the Zn(II) content of the resulting apoenzyme.[24]

Preparation of Co(II)-Substituted IMP-1 by Direct Addition. Metal-free IMP-1, as confirmed by ICP-AES measurements, was concentrated to ca. 1 mM by ultrafiltration. The concentrated enzyme was then centrifuged (10 min at 14000*g*) to remove precipitated protein. $CoCl_2$ (1−2 mol equiv) (Strem Chemicals, 99.999% pure) was added, and the mixture was incubated for 20−30 min in ice. The resulting enzyme was pink in color and remained pink for weeks when stored at −80 °C.

UV−vis Spectroscopy of Co(II)-Substituted IMP-1. UV−vis spectra were obtained on a Hewlett−Packard 5480A UV−vis spectrophotometer measuring the absorbance between 200 and 800 nm at 25 °C. Background spectra of apo-IMP-1 were used to generate difference spectra of the Co(II)-substituted samples.

EPR Spectroscopy on Co(II)-Substituted IMP-1. EPR spectroscopy at cryogenic temperatures was carried out using a Bruker EleXsys E600 spectrometer equipped with an Oxford Instruments ESR900 helium flow system and an ITC503 temperature controller. EPR spectra were recorded at 9.63 GHz using an ER4116DM cavity operating in TE_{102} (perpendicular) mode, with 4096 data points collected over 8000 G, and 4 G magnetic field modulation at 100 kHz. An integral microwave counter provided precise microwave frequencies that were found to vary within 0.0025 GHz among the samples examined, and resonance position reproducibility was measured to be ±2 G. Spectra were recorded over 180 s, and other acquisition parameters were chosen such that resolution and reproducibility were limited by the modulation amplitude. The temperatures and microwave powers for individual spectra are given in the legend to Figure 5.

RESULTS

Overexpression, Purification, and Characterization of Recombinant IMP-1. Recombinant IMP-1 was overexpressed and purified using the procedure of Laraki et al.,[30] except that 50 μM $ZnSO_4$ was not included in the 50 mM HEPES (buffer A) and the previously reported MonoS chromatographic step was not performed. By using the procedure described in the Experimental Procedures section, high levels of purified IMP-1 were obtained. IMP-1 eluted from the SP-Sepharose column between 225 and 250 mM NaCl. The overall yield of purified IMP-1 ranged between 10 and 15 mg/L of culture, and the purity of IMP-1 was ascertained by SDS-PAGE to be greater than 95%. Metal analyses of recombinant IMP-1 indicated the enzyme binds 2.0 ± 0.3 equiv of Zn(II), and this sample was called recombinant IMP-1. MALDI-TOF mass spectrometry demonstrated that recombinant IMP-1 exhibits an m/z of 25 113, which is in good agreement with the molecular weight reported by Laraki et al. of 25 103 m/z[30] and from the deduced amino acid sequence (25 111 amu).[7] The catalytic activity of recombinant IMP-1 was evaluated using nitrocefin as a substrate. Steady-state kinetic studies revealed a k_{cat} of 135 ± 14 s^{-1} and a K_m of 28 ± 12 (Table 1).

Table 1. Steady-State Kinetics Parameters of Recombinant IMP-1[a]

	experimental	calculated
K_m (μM)	28 ± 12	30
k_{cat} (s^{-1})	135 ± 14	116

[a]The experimental values were determined by monitoring the hydrolysis of nitrocefin in 50 mM HEPES, pH 7.5, and 25 °C. The calculated values were determined by using the theoretical equations for k_{cat} and K_m, given the reaction mechanism shown in Scheme 1(2), as determined by the King−Altman method.

Stopped-Flow Kinetic Studies on IMP-1. In an effort to probe the kinetic mechanism of recombinant IMP-1 for the hydrolysis of β-lactam antibiotics, nitrocefin was used as a substrate. Diode-array UV−vis spectra of 35 μM recombinant IMP-1 reacted with 35 μM nitrocefin were monitored over a 1000 ms time period between 300 and 700 nm. Two distinct absorbance features were identified: (1) a broad absorption band at 390 nm (corresponds to unhydrolyzed substrate) that decreased over time and (2) a broad absorption band at 485 nm (corresponds to hydrolyzed nitrocefin) that increased over time (Figure 1). There was no evidence of an additional peak at 665 nm (corresponding to an anionic intermediate) that was previously reported in similar studies with L1,[25] IMP-1,[31] and CcrA[32] but absent in studies on BcII[33] and Bla2.[19]

To further investigate the reaction mechanism of recombinant IMP-1 with nitrocefin, stopped-flow kinetic studies were conducted under near single turnover conditions using 35 μM IMP-1 with 35 μM nitrocefin (Figure 2a). Progress curves of substrate and product in Figure 2a were fitted to three possible reaction mechanisms (Scheme 1). Algebraic expressions for k_{cat}

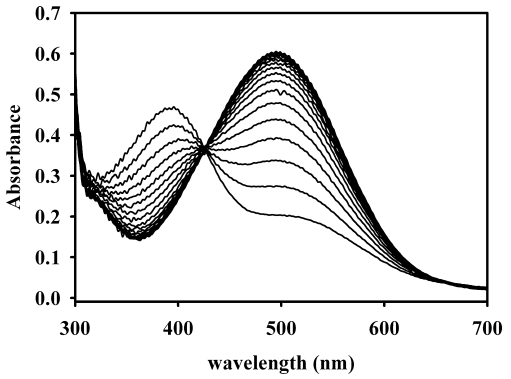

Figure 1. Diode-array UV−vis spectra of the reaction of 35 μM IMP-1 with 35 μM nitrocefin in 50 mM HEPES, pH 7.5, at 4 °C. Spectra were obtained every 20 ms.

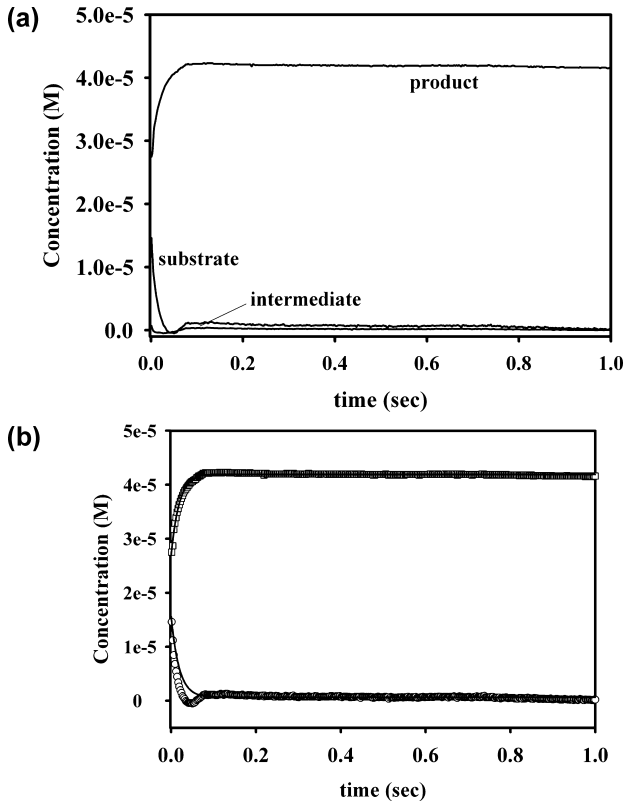

Figure 2. (a) Stopped-flow kinetics of the hydrolysis of nitrocefin by recombinant IMP-1. Concentrations of product, substrate, and intermediate were calculated as previously reported.[25] (b) Theoretical progress curves (lines) drawn over the experimental stopped-flow kinetic data of recombinant IMP-1. The kinetic mechanism in Scheme 1(1) and the rate constants—$k_1 = 10^8$ M^{-1} s^{-1}, $k_{-1} = 3.0 \times 10^3$ s^{-1}, $k_2 = 20$ s^{-1}, $k_{-2} = 2.6 \times 10^{-1}$ s^{-1}, $k_3 = 3.3 \times 10^3$ s^{-1}, and $k_{-3} = 10^8$ M^{-1} s^{-1}—were used to simulate the kinetic data.

and K_m values for each mechanism using the King−Altman method[26] were used validate the best fits. While many values of the microscopic rate constants yielded calculated progress curves that matched the experimental data, the simplest scheme that adequately fitted the data and that provided theoretical k_{cat} and K_m similar to the experimental values is given in Scheme 1(1). Kinetic data and simulations indicate IMP-1 follows the simplest mechanism by which cleavage of the C−N β-lactam bond is rate-limiting. The calculated theoretical values (k_{cat} =116 s^{-1}, K_m = 30 μM) are in excellent agreement with experimental values (Table 1). In further support of this kinetic mechanism, we found that 38 μM hydrolyzed nitrocefin inhibited by 76% the IMP-1-catalyzed hydrolysis of nitrocefin (data not shown).

EXAFS Spectroscopic Studies on IMP-1. EXAFS spectra were collected to probe (1) metal coordination number, (2) metal−ligand and metal−metal distances, and (3) amino acid ligand identity in recombinant IMP-1. EXAFS spectra were collected on three independently prepared samples of recombinant IMP-1. Fourier-transformed EXAFS data for recombinant IMP-1 (Figure 3 and Figure S1) were best fitted

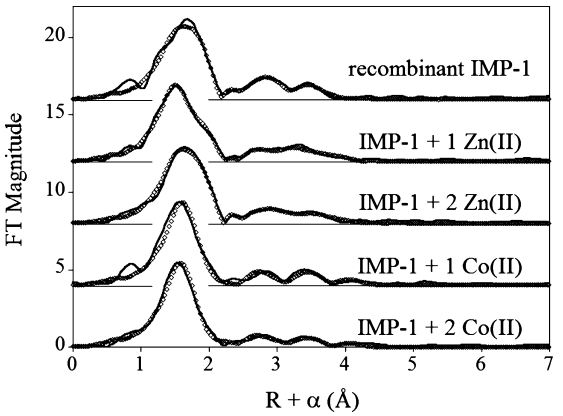

Figure 3. Fourier-transformed EXAFS of Zn(II)- and Co(II)-containing IMP-1 (solid lines) and corresponding best fits (open symbols). See Table 2, Tables S1−S3, and Figures S1−S5 for details.

with a mixed first shell of 4N/O + 0.5S + 0.5C (from a coordinated carboxylate). Inclusion of the sulfur scatterer reduced the first shell fit residual more than 4-fold, while addition of the carbon path further reduced it another factor of 2 (see Table S1). Multiple-scattering fits indicate an average of 2 His ligands per Zn(II) ion. Inclusion of a Zn−Zn vector improved the fit residual by nearly 60%. The refined Zn−Zn distance of 3.39 Å is in good agreement with the metal−metal separation of 3.3 Å reported by Yamaguchi et al.[16] The crystal structure of recombinant IMP-1[16] indicates the metal binding site is representative of a class B1MβL, with the Zn_1 site composed of three His ligands and the Zn_2 site defined by one His, one Cys, one Asp, and a terminal water ligand. The two metals are bridged by a solvent molecule, leading to an average Zn site of 4N/O + 0.5S donors, including 2 His ligands per Zn(II), and the EXAFS are consistent with this picture (Table 2). The metal−ligand distances determined by EXAFS are all in reasonable agreement with those reported in the crystal structure.

Preparation and Characterization of Co(II)-Substituted IMP-1 by Direct Addition. In order to structurally characterize IMP-1 further, Co(II)-substituted analogues were prepared and characterized. Two direct addition methods were attempted in preparing Co(II)-substituted IMP-1. The initial step in each method required the preparation of metal-free enzyme. Chelators 1,10- phenanthroline and EDTA were used during this step. The use of 1,10-phenanthroline resulted in substantial precipitation of dilute (20 μM) and concentrated (ca. 1 mM) samples after the first dialysis step. As a result, EDTA was used in all remaining preparations of metal-free

dx.doi.org/10.1021/bi200839h | Biochemistry 2011, 50, 9125−9134

Table 2. Best Fits to EXAFS of Zn(II) and Co(II)-Containing IMP-1[a]

model	M−N/O	M−S	M−C	M−His[b]	M−M
recombinant IMP-1					
4N/O (2 His) + 0.5S + 0.5C + Zn−Zn	2.03 (5.7)	2.26 (0.9)	2.53 (0.1)	2.95 (6.0), 3.25 (11), 4.14 (9.4), 4.46 (19)	3.39 (8.1)
IMP-1 with 1 Zn(II)					
4N/O (2 His) + 0.5S + 0.5C + Zn−Zn	2.00 (5.0)	2.26 (1.0)	2.54 (1.2)	2.89 (4.9), 3.11 (4.6), 4.02 (8.0), 4.42 (6.6)	
IMP-1 with 2 Zn(II)					
4N/O (2 His) + 0.5S + 0.5C + Zn−Zn	2.02 (5.9)	2.27 (0.9)	2.52 (0.1)	2.93 (7.6), 3.34 (8.4), 4.15 (12), 4.47 (9.0)	3.39 (14)
IMP-1 with 1 Co(II)					
4N/O (2 His) + 0.5S + Co−Co	2.09 (2.5)	2.33 (2.8)		2.82 (19), 3.16 (8.2), 4.16 (0.5), 4.56 (9.4)	3.42 (13)
IMP-1 with 2 Co(II)					
4N/O (2 His) + 0.5S + Co−Co	2.08 (2.3)	2.33 (1.8)		2.93 (23), 3.15 (8.5), 4.17 (0.9), 4.59 (11)	3.45 (15)

[a]Distances (Å) and disorder parameters (in parentheses, σ^2 (10^{-3} Å^2)) shown derive from integer or half-integer coordination number fits to filtered EXAFS data [Δk = 1.5−13 Å^{-1} (Zn) or 1.5−12.4 Å^{-1} (Co); ΔR = 0.3−4.3 Å]. See Tables S1−S3 and Figures S1−S5 for detailed fits. [b]Multiple scattering paths represent combined paths, as described previously (see Experimental Procedures).

Table 3. Steady-State Kinetic Constants of IMP-1 Analogues Made by Direct Addition of Metal to Apo-IMP-1

	recombinant IMP-1	IMP-1 with 1 Co(II)	CoCo−IMP-1	IMP-1 with 1 Zn(II)	ZnZn−IMP-1
K_m (μM)	28 ± 12	12 ± 5	25 ± 7	18 ± 5	29 ± 7
k_{cat} (s^{-1})	135 ± 14	35 ± 4	105 ± 10	70 ± 7	113 ± 11
k_{cat}/K_m (μM^{-1} s^{-1})	4.8	2.9	4.2	3.9	3.9

IMP-1, following the procedure described in Experimental Procedures. ICP-AES measurements on multiple apo-IMP-1 samples demonstrated undetectable levels of Zn, Co, Fe, or Mn.

Apo-IMP-1 samples were concentrated to ca. 1 mM by ultrafiltration. The concentrated enzyme was then centrifuged to remove precipitated protein. $CoCl_2$ or $ZnCl_2$ (1−2 mol equiv) was added, and the mixture was incubated for 20−30 min on ice. The Co(II)-treated enzyme was pink in color and remained pink for weeks when stored at −80 °C.

Steady-State Kinetics of Metal-Substituted IMP-1. To ascertain the catalytic activity of the metal-substituted enzymes (IMP-1 samples containing 1 or 2 equiv of Zn(II) and Co(II)), steady-state kinetic constants were determined using nitrocefin as a substrate in 50 mM HEPES, pH 6.8, and the resulting values were compared to those of as-isolated, ZnZn-IMP-1 (Table 3). The samples containing 1 equiv of Zn(II) or Co(II) exhibited roughly 50% the activity of the dinuclear enzymes. The K_m values exhibited by the three dinuclear forms (as-isolated-, ZnZn-, and CoCo-IMP-1) were identical within error, while the K_m values of the samples containing 1 equiv of Zn(II) and Co(II) were slightly lower. There was a slight decrease in k_{cat} values of the metal-added samples as compared to that of the as-isolated enzyme, most likely due to small amounts of protein being denatured as metal ion stocks are added to the apoenzyme.

Spectroscopic Characterization of Co(II)-Substituted IMP-1. UV−vis difference spectra (spectra of the Co-bound samples minus the spectrum of apo-IMP-1) were obtained for the IMP-1 analogues containing 1 and 2 equiv of Co(II). The addition of 1 equiv of Co(II) to apo-IMP-1 resulted in a broad absorption peak at 340 nm and additional peaks between 500 and 600 nm (Figure 4). The feature observed near 340 nm ($\varepsilon_{340\,nm}$ = 155 M^{-1} cm^{-1}) is assigned to a Cys-S Co(II) ligand-to-metal charge transfer transition,[23,32,34] which strongly suggests cobalt binding at the consensus Zn_2 site. In addition,

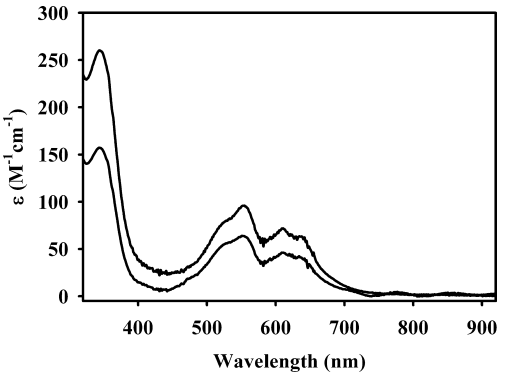

Figure 4. UV−vis difference spectra of IMP-1 containing 0.9 equiv of Co(II) (bottom spectrum) and 1.9 equiv of Co(II) (top spectrum). The enzyme concentration was 0.840 mM in 50 mM HEPES, pH 6.8, containing 0.5 M NaCl.

the broad peak at 550 nm ($\varepsilon_{550\,nm}$= 63 M^{-1} cm^{-1}) is assigned to ligand field transitions of high-spin Co(II).[35] The magnitudes of the extinction coefficient of these peaks suggest a ligand coordination number of 5/6. The addition of a second equivalent of Co(II) to the sample results in a spectrum showing an increase in the intensities of both features ($\varepsilon_{550\,nm}$= 95 M^{-1} cm^{-1}, $\varepsilon_{340\,nm}$= 256 M^{-1} cm^{-1}). These results suggests Co(II) is distributed between both binding sites in both Co(II)-containing samples.

EXAFS studies were conducted on Zn(II)- and Co(II)-reconstituted analogues of IMP-1 (Figure 3 and Figures S2−S5; Table 2 and Table S2). For IMP-1 containing 1 equiv of Zn(II) (Figure S2 and Table S2), the EXAFS data are best fitted with a mixed first shell of 4N/O + 0.5S + 0.5C. Inclusion of the sulfur path reduced the fit residual by 88%, while addition of the Zn−C path decreased it 64% further, suggesting both a sulfur (Cys) and a carboxylate carbon are part of the primary coordination sphere of the first added equivalent of zinc. Multiple-scattering fits indicate an average of 2 histidines per Zn, which suggests

dx.doi.org/10.1021/bi200839h | Biochemistry 2011, 50, 9125−9134

that the first equivalent of Zn(II) is distributed between the two binding sites. Addition of Zn−Zn scattering path did not significantly improve the fit residual (only 12%), and it refined to an unreasonably short distance of 3.23 Å, indicating the lack of a metal−metal interaction with one added equivalent of Zn(II). These data do not indicate cooperativity in Zn(II) binding. Addition of a second equivalent of Zn(II) leads to a model that is indistinguishable from that obtained for recombinant IMP-1 (Figure S3 and Table S2).

In contrast, EXAFS data of IMP-1 with 1 equiv of added Co(II) (Figure 3 and Figure S4, Table 2 and Table S3) are best fitted with a model that appears to indicate an intact dinuclear cluster. The model includes 4N/O + 0.5S ligands in the primary coordination sphere, without showing evidence of the carboxylate carbon. Multiple-scattering fits indicate an average of 2 histidines per Co(II), and inclusion of a Co−Co vector reduces the fit residual by 33%, refining to a reasonable distance of 3.42 Å. The same model produced the best fit to the EXAFS data for IMP-1 containing 2 equiv of added Co(II) (Figure 3 and Figure S5, Table 2 and Table S3), including a Co−Co distance of 3.45 Å that led to a 39% decrease in the fit residual. The Co−Co distance for IMP-1 containing 2 added equivalents of Co(II) is slightly longer than that obtained with 1 added equivalent of Co(II) (3.45 Å vs 3.42 Å). In both cases, the average Co−N/O distance is ca. 0.06−0.08 Å longer than the corresponding Zn−N/O distance, which may reflect an increase in average coordination number for Co(II).

The EPR spectrum of IMP-1 containing 1 equiv of Co(II) exhibited a complex $S = {}^3/_2$, $M_S = |\pm{}^1/_2\rangle$ signal that was unsaturated at 8 K and 0.2 mW but could not be simulated as a single species (Figure 5A). This result indicated at least two distinct Co(II) species, each either 5- or 6-coordinate.[36] Some barely resolved ^{59}Co hyperfine structure was observed on the maximum feature at around 1300 G (130 mT), but the lines were otherwise broad, suggesting coordination by one or more solvent molecules in addition to the protein-derived ligands. Spectra of IMP-1 containing 1 equiv of Co(II) at different pH values (Figure 5A−C) suggested a pH-dependent equilibrium between at least two species, one of which exhibited some ^{59}Co hyperfine splitting of the low field absorption (1000−1500 G; 100−150 mT) at the higher pH values (compare traces A−C of Figure 5) with $A(^{59}\text{Co}) \sim 6.5 \times 10^{-3}$ cm^{-1}. This result may indicate either a Co−OH/Co−OH$_2$ equilibrium or else a pH-dependent mixture of a 5- and 6-coordinate species that differ in the number of coordinated solvent molecules. At higher microwave power and lower temperature (5.5 K, 100 mW), the $M_S = |\pm{}^1/_2\rangle$ signal was distorted by rapid-passage effects, and an additional, faster-relaxing narrow absorption feature at 1050 G (105 mT, $g_{\text{eff}} = 6.5$) was detectable, characteristic of an $M_S = |\pm{}^3/_2\rangle$ signal and due to tetrahedral Co(II) (Figure 5B). Interestingly, the rapid passage effects on the $M_S = |\pm{}^1/_2\rangle$ signal appeared to be more apparent at lower pH, suggesting that lower pH favors 6-coordinate rather than 5-coordinate Co(II). The intensity of the $M_S = |\pm{}^3/_2\rangle$ signal relative to the $M_S = |\pm{}^1/_2\rangle$ signal increased with increasing pH, again suggesting that lower coordination numbers are favored at higher pH values, whereas lower pH values favor higher coordination, presumably due to additional coordination by solvent molecules. Upon addition of a second Co(II) ion, the enzyme yields a spectrum (Figure 5C) under nonsaturating conditions that is higher in intensity than that of IMP-1 containing 1 equiv of Co(II) but otherwise similar to, though not superimposable with, that of IMP-1 containing 1 equiv of Co(II). A difference spectrum (Figure 5E) indicates that upon addition of the second Co(II) ion the amount of a broad $M_S = \pm{}^1/_2$ axial species, devoid of resolved ^{59}Co hyperfine structure and with no well-resolved g'_z feature, increases relative to that of the second species with resolved g' resonances and partially resolved ^{59}Co hyperfine structure. It is unclear whether the species that is more dominant at higher levels of Co(II) is due to a distinct 5- or 6-coordinate Co(II) ion with solvent coordination or whether the poor resolution of g' resonances and lack of hyperfine structure is a consequence of dipolar broadening due to Co(II)−Co(II) interactions in dinuclear centers. Parallel mode studies in the TE$_{012}$ cavity mode showed no evidence for the weak exchange coupling that is often observed for dinuclear Co(II) centers in substituted dinuclear metallohydrolases,[36] but some dipolar coupling is to be expected. The magnitude of the dipolar interaction is likely small compared to the line width for the $M_S = \pm{}^1/_2$ signals, and the precise effect on the spectra is sensitive to the relative orientations of the **g**-tensors and the interspin vector[37] and will differ in individual molecules depending on the precise nature of the electronic structure of the two Co(II) ions which, in turn, will depend on chemical factors such as the degree of solvent coordination and the protonation state of coordinated solvent. Detailed pH dependence and ^{1}H electron−nuclear double resonance studies will be required to address further the natures of the putative species and their equilibria. Some information, however, is available from the spectrum of IMP-1 with two added Co(II) ions, recorded at 5.5 K and 100 mW (Figure 5D). The spectrum suggests that the tetrahedral ($M_S = \pm{}^3/_2$) site is filled, on aggregate, before the higher coordinate site, indicating that the cooperativity of Co(II) binding to IMP-1, while substantial, is not absolute. These data for IMP-1 contrast markedly with those from another B1 enzyme, CcrA.[21] In that enzyme, the binding is highly sequential, and the two distinct sites each exhibit EPR, EXAFS, and optical absorption spectra that indicate 5- or 6-fold

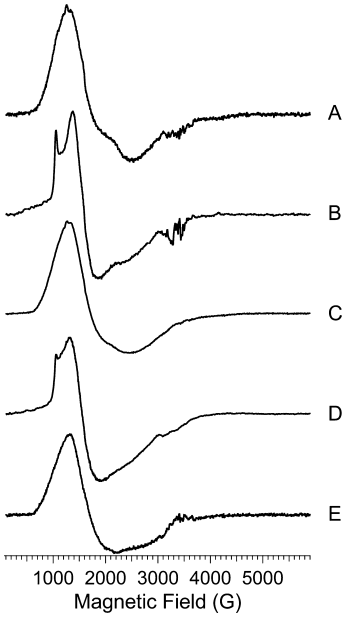

Figure 5. Experimental EPR spectra of Co(II)-containing IMP-1: (A) IMP-1 containing 1 equiv of Co(II), 0.2 mW, 13K; (B) IMP-1 containing 1 equiv of Co(II), 100 mW, 5K; (C) CoCo-IMP-1, 0.2 mW, 13K; (D) CoCo-IMP-1, 100 mW, 5K. (E) Difference spectrum, CoCo-IMP-1 minus IMP-1 containing 1 equiv of Co(II), 0.2 mW, 13K.

coordination of Co(II), presumably due to additional solvent coordination, whereas a tetrahedral site and positively cooperative binding are indicated in IMP-1.

DISCUSSION

Bacterial resistance to antibiotics is an alarming medical crisis.[38] The misuse of current antibiotics and the rapid dissemination of resistance genes via conjugation/horizontal gene transfer have resulted in infections, once treated with inexpensive antimicrobial agents, that are no longer treatable. The largest class of antibiotics is the β-lactam containing agents; however, the emergence and spread of certain β-lactamases have made many of these β-lactam containing antimicrobial agents not as effective as in the past.[3,39] IMP metallo-β-lactamases (and variants) are one such group of β-lactamases that hydrolyze almost all known β-lactam-containing antibiotics.[8] The genes for the IMP variants readily transfer among other bacterial strains, thereby reducing the number of β-lactam susceptible strains. One strategy to combat β-lactam resistance is to utilize antibiotics from other classes, such as the quinolones and macrolides. Unfortunately, clinical resistance to these alternative antibiotics is already evident, leaving very few options to treat bacterial infections.[1] A second strategy that has been used previously to combat β-lactam resistance, specifically caused by certain serine-β-lactamases, is the production of β-lactamase inhibitors, such as tazobactam and clavulanic acid.[40] These inhibitors are given in combination with existing β-lactam containing antibiotics to combat resistant bacterial strains. Unfortunately, none of the existing β-lactamase inhibitors can be used in the clinic to combat metallo-β-lactamases like IMP-1. Therefore, there is considerable interest in identifying clinically useful inhibitors against the metallo-β-lactamases.[8,15,41−47] One strategy to prepare these inhibitors is to structurally and mechanistically characterize the enzymes in an effort to rationally design inhibitors. In studies on L1 and ImiS, spectroscopic studies, in combination with rapid freeze quench technology and Co(II)-substituted analogues of the enzymes, have been used to interrogate the mechanism as substrate is converted to product.[20,48,49] The first step in conducting these spectroscopic studies is to successfully prepare active, well-characterized Co(II)-substituted analogues of the native Zn(II)-containing enzyme. This work describes our efforts at preparing and characterizing the Co(II)-substituted analogue of IMP-1.

The overexpression and purification of recombinant IMP-1 have been reported by several groups, and the purification procedures, when specified, involved multiple chromatographic steps.[5,30,41,50−52] The purification of IMP-1 presented herein required a single chromatographic step, and protein yields were similar to those reported earlier. The k_{cat} value of recombinant IMP-1 (Table 1) was 2-fold higher than reported by Laraki but 1.4-fold lower, after normalizing for different assay temperatures, than the values reported by others.[30,45,51,52] The higher k_{cat} (and corresponding k_{cat}/K_m) values reported by Siemann,[45] Materon,[51] and Oelschlaeger[52] were obtained in assays that contained 50−100 μM Zn(II) and bovine serum albumin, and both of these additives likely maintained larger amounts of active ZnZn−IMP-1. The K_m value of recombinant IMP-1 (Table 1) is identical to that reported by Laraki, but 2−3-fold larger than previously reported by others.[30,45,51,52] Our larger values for K_m are likely due to our excluding extra Zn(II) in the IMP-1 samples used in our steady-state kinetic assays, as previously observed in studies with L1.[24] The metal content of recombinant IMP-1 purified as described in Experimental Procedures was 2 equiv, which is similar to that reported by Laraki.[30] Many of the other reports of overexpression and purification of IMP-1 did not report metal content. Differing buffers and pH's[9,45,52] and added Zn(II) (and bovine serum albumin) in assay buffers[51,52] undoubtedly contributed to the differences in the steady-state kinetics.

β-Lactamase hydrolysis of the β-lactam ring involves two steps: a nucleophilic attack on the carbonyl group and C−N bond cleavage; however, these reactions may be concerted in some enzymes.[53] Previous mechanistic studies on dinuclear MβLs CcrA and L1, using nitrocefin as a substrate, concluded that the rate-limiting step was protonation of anionic, ring-opened intermediate formed during catalysis.[25,54] Similar kinetic studies on Bla2 and BcII showed that the nitrocefin-derived reaction intermediate was not observed,[19,33] and Vila suggested that the absence of this intermediate might be due to the relatively short loop that covers BcII's active site.[33] Similar studies on IMP-1 are conflicting. Moali et al. reported that small amounts of intermediate were formed and that the reaction rate was so fast that it was difficult to accumulate significant amounts of the intermediate.[31] On the basis of these results, Moali suggested a kinetic mechanism similar to those of L1 and CcrA and reported the simulated rate constants based on that mechanism. On the other hand, Yamaguchi et al. reported that no intermediate is formed.[16] In the present study, stopped-flow kinetic studies were conducted on IMP-1 in an effort to resolve the conflicting data. There was no peak at 665 nm, corresponding to a reaction intermediate, observed in our data (Figure 1), and we could not detect a peak by lowering the temperature of the water bath or by varying the enzyme and substrate concentrations (data not shown). Therefore, we conclude that the anionic intermediate, previously observed in studies on L1 and CcrA,[25,54] is not observed in the rapid kinetic studies on recombinant IMP-1, consistent with results reported by Yamaguchi.[16] The rapid kinetic data on recombinant IMP-1 was simulated using a simple Michaelis kinetic scheme,[26] and microscopic rate constants are reported. Importantly, this scheme was used to derive theoretical kinetic constants, and the resulting theoretical values (Table 1) for k_{cat} and K_m are very similar to those determined from experiments. Since the loop in IMP-1 is relatively larger than that in BcII,[55] the loop alone cannot explain the absence of the anionic intermediate in the enzymes. An examination of several MβL active sites shows subtle differences in the positions of metal binding ligands and major differences in nonmetal binding regions around the metal binding sites. In fact, the regions around the metal binding sites in L1 and CcrA, both of which stabilize the anionic intermediate, are very different. It is clear that presence of the reactive intermediate must be accompanied by precise orientations of ligands around the active site.[56]

Compared to L1, CcrA, ImiS, and BcII, there have been very few spectroscopic studies reported on IMP-1 or on any of the IMP variants. This lack of data could possibly be due to the inability to reconstitute apo-IMP-1 with metal ions.[30,45,57] By using the procedure as described in Experimental Procedures, Co(II)-substituted IMP-1 and reconstituted ZnZn−IMP-1 can now be prepared and used in spectroscopic studies. EXAFS studies were conducted on the as-isolated ZnZn−IMP-1 so that these results could be compared to those on the metal-reconstituted samples. The EXAFS data yielded metal−metal and metal−ligand distances that are in excellent agreement with those previously reported in crystal structures.[14,16] In addition,

EXAFS studies on reconstituted ZnZn−IMP-1 yielded identical values for metal−metal and metal−ligand distances, which demonstrates that the metal-reconstitution/substitution method described herein yields the same enzyme as isolated, which is supported by the steady-state kinetic studies (Table 3).

The direct addition of Co(II) or Zn(II) to apo-MβLs can result in three possible metal binding modes: (1) sequential (metal binds to the Zn_1 site and then to the Zn_2 site; activity is variable depending on the activity of the mononuclear enzyme, (2) positive cooperative (the binding of the first metal equivalent increases the affinity for the binding of a second equivalent of metal: addition of 1 equiv of metal results in a mixture of 50% apoenzyme and 50% fully loaded enzyme and in roughly 50% activity; (3) random (the metal distributes between both sites; very difficult to predict the activity of the resulting mixture). Steady-state kinetics were conducted prior to the spectroscopic studies to confirm that the Co(II)-substituted analogues retain catalytic activity (Table 3). The mono- and binuclear analogues of IMP-1 all exhibited activity (Table 3). In general, the steady-state kinetic studies suggest that metal binding to IMP-1 follows a positive cooperative mode. IMP-1 containing 1 equiv of Zn(II) exhibits a k_{cat} that is roughly 50% of that for the as-isolated enzyme. IMP-1 containing 1 equiv of Co(II), however, exhibits a k_{cat} that is only 33% of that for the CoCo−IMP-1 analogue. This lower k_{cat} for IMP-1 containing 1 equiv of Co(II) is probably due to some oxidation of the Co(II) after adding the metal to the dilute apoenzyme sample. This lower k_{cat} value for IMP-1 containing 1 equiv of Co(II) probably explains why this analogue's k_{cat}/K_m value is lower than that of the other analogues (Table 3). The K_m values, which have been confirmed with at least 10 different preparations of the analogues, for the IMP-1 analogues containing only 1 equiv of metal ion are significantly lower than those for the analogues containing 2 equiv of metal ions (Table 3). This result is not expected for positive cooperative binding of metal, which would result in a K_m value that is identical to that of the dinuclear metal ion containing analogue. We currently do not know why the analogues containing 1 equiv of metal ion exhibit lower K_m values; however, it may be due to the relatively low concentrations of the enzyme (10−30 nM) with respect to the concentration of adventitious Zn(II) in our buffers (100−200 nM).[20] Wommer et al. previously hypothesized that substrate activates the binding of Zn(II);[58] therefore, it is possible that a substrate−Zn(II) complex could bind better to the apoenzyme, resulting in an apparent lower value for K_m.

Spectroscopic studies on IMP-1 support positive cooperative binding of Co(II) to the enzyme. UV−vis spectroscopy on Co(II)-substituted IMP-1 revealed two distinct absorbance peaks with the addition of 1−2 equiv to apo-IMP-1 (Figure 4). The feature observed near 340 nm is attributed to a ligand (Cys-S) to metal charge transfer band. Cys221, in the concensus Zn_2 site,[13,59] coordinates Co(II) when 1 equiv of the metal binds, and Cys-S coordination increases as the second equivalent of Co(II) is added. EXAFS spectra on IMP-1 containing 1 equiv of Co(II) are best fitted including a metal−metal contribution, suggesting that metal ions occupy both the Zn_1 and Zn_2 sites in the enzymes containing only 1 equiv of metal ion. While the EXAFS fits did not significantly improve with including a metal−metal interaction for IMP-1 containing 1 equiv of Zn(II), it is very likely that this sample also exhibits positive cooperativity, given the steady-state kinetic data (Table 3). Likewise, EPR spectra on Co(II)-substituted IMP-1 samples strongly support positive cooperative metal binding to IMP-1. These results suggest that there are mixtures of fully loaded and apo-IMP-1 upon addition of 1 equiv of metal ion.

Previous studies on other MβLs have shown that CcrA exhibits positive cooperative[60] or sequential[61] Zn(II) binding and sequential Co(II) binding.[21] L1[20] and Bla2[19] exhibit mostly sequential and sequential/distributed metal binding, respectively. Reports dealing with metal binding to BcII have varied substantially with several groups reporting sequential binding[23,62−66] and one group reporting noncooperative Zn(II) binding with a subsequent dimerization of the enzyme.[67] Another report on BcII suggested positive cooperative binding,[68] and several groups have recently reported that the only active form of BcII is the dinuclear metal ion containing form,[69−71] suggesting positive cooperative binding. Careful titration of BcII with Co(II) has demonstrated mixtures of apo-, mono-, and dinuclear metal ion containing forms, even in the presence of low levels of Co(II).[72] These latter studies suggest a complex equilibrium process for metal binding to BcII but favor, in part, some positive cooperative Co(II) binding to BcII. The data presented herein suggest that IMP-1 exhibits positive cooperative binding of both Zn(II) and Co(II). The ability to prepare metal-substituted analogues of IMP-1 will now allow for future rapid-freeze quench spectroscopic studies to probe the reaction mechanism of the enzyme. Information gleaned from these studies will allow for the design of mechanism-based inhibitors.

■ ASSOCIATED CONTENT

Ⓢ Supporting Information

EXAFS spectra and fitting data on recombinant IMP-1 and IMP-1 with 1 and 2 equiv of added Zn(II) or Co(II). This material is available free of charge via the Internet at http://pubs.acs.org.

■ AUTHOR INFORMATION

Corresponding Author

*E-mail: crowdemw@muohio.edu. Phone: (513) 529-7274. Fax: (513) 529-5715.

Funding

This work was supported by the National Institutes of Health (EB001980 to the Medical College of Wisconsin; GM093987 to M.W.C. and D.L.T.), Miami University/Volwiler Professorship (to M.W.C.).

■ ABBREVIATIONS

EDTA, ethylenediaminetetraacetic acid; HEPES, 4-(2-hydroxymethyl)-1-piperazineethanesulfonic acid; ICP-AES, inductively coupled plasma with atomic emission spectroscopy; IPTG, isopropyl β-D-thiogalactoside; LB, Luria−Bertani.

■ REFERENCES

(1) Gupta, V. (2008) Metallo β-lactamases in *Pseudomonas aeruginosa* and *Acinetobacter* species. *Expert Opin. Invest. Drugs 17*, 131−143.

(2) Perez, F., Endimiani, A., Hujer, K. M., and Bonomo, R. A. (2007) The continuing challenge of ESBLs. *Curr. Opin. Pharmacol. 7*, 459−469.

(3) Walsh, T. R., Toleman, M. A., Poirel, L., and Nordmann, P. (2005) Metallo-β-lactamases: the quiet before the storm? *Clin. Microbiol. Rev. 18*, 306−325.

(4) Yong, D., Toleman, M. A., Giske, C. G., Cho, H. S., Sundman, K., Lee, K., and Walsh, T. R. (2009) Characterization of a new metallo-β-

lactamase gene, blaNDM-1, and a novel erythromycin esterase gene carried on a unique genetic structure in *Klebsiella pneumoniae* sequence type 14 from India. *Antimicrob. Agents Chemother. 53*, 5046−5054.
(5) Osano, E., Arakawa, Y., Wacharotayankun, R., Ohta, M., Horii, T., Ito, H., Yoshimura, F., and Kato, N. (1994) Molecular Characterization of an Enterobacterial Metallo-β-Lactamase Found in a Clinical Isolate of *Serratia marcescens* That Shows Imipenem Resistance. *Antimicrob. Agents Chemother. 38*, 71−78.
(6) Watanabe, M., Iyobe, S., Inoue, M., and Mitsuhashi, S. (1991) Transferable Imipenem Resistance in *Pseudomonas aeruginosa*. *Antimicrob. Agents Chemother. 35*, 147−151.
(7) Laraki, N., Galleni, M., Thamm, I., Riccio, M. L., Amicosante, G., Frere, J. M., and Rossolini, G. M. (1999) Structure of In31, a blaIMP-containing *Pseudomonas aeruginosa* integron phyletically related to In5, which carries an unusual array of gene cassettes. *Antimicrob. Agents Chemother. 43*, 890−901.
(8) Oelschlaeger, P., Ai, N., DuPrez, K. T., Welsh, K. J., and Toney, J. H. (2010) Evolving carbapenemases: Can medicinal chemists advance one step ahead of the coming storm? *J. Med. Chem. 53*, 3013−3027.
(9) Iyobe, S., Kushadokoro, H., Ozaki, J., Matsumura, N., Minami, S., Haruta, S., Sawai, T., and O'Hara, K. (2000) Amino Acid Substitutions in a Variant of IMP-1 Metallo-β-Lactamase. *Antimicrob. Agents Chemother. 44*, 2023−2027.
(10) Yano, H., Kuga, A., Okamoto, R., Kitasato, H., Kobayashi, T., and Inoue, M. (2001) Plasmid-Encoded Metallo-β-Lactamase (IMP-6) Conferring Resistance to Carbapenems, Especially Meropenem. *Antimicrob. Agents Chemother. 45*, 1343−1348.
(11) Iyobe, S., Kusadokoro, H., Takahashi, A., Yomoda, S., Okubo, T., Nakamura, A., and O'Hara, K. (2002) Detection of a Variant Metallo-β-Lactamase, IMP-10, from Two Unrelated Strains of *Pseudomonas aeruginosa* and an *Alcaligenes xylosoxidans* Strain. *Antimicrob. Agents Chemother. 46*, 2014−2016.
(12) Docquier, J. D., Riccio, M. L., Mugnaioli, C., Luzzaro, F., Endimiani, A., Toniolo, A., Amicosante, G., and Rossolini, G. M. (2003) IMP-12, a new plasmid-encoded metallo-β-lactamase from a *Pseudomonas putida* clinical isolate. *Antimicrob. Agents Chemother. 47*, 1522−1528.
(13) Crowder, M. W., Spencer, J., and Vila, A. J. (2006) Metallo-β-lactamases: Novel weaponry for antibiotic resistance in bacteria. *Acc. Chem. Res. 39*, 721−728.
(14) Concha, N. O., Janson, C. A., Rowling, P., Pearson, S., Cheever, C. A., Clarke, B. P., Lewis, C., Galleni, M., Frere, J. M., Payne, D. J., Bateson, J. H., and Abdel-Meguid, S. S. (2000) Crystal Structure of the IMP-1 Metallo-β-Lactamase from *Pseudomonas aeruginosa* and Its Complex with a Mercaptocarboxylate Inhibitor: Binding Determinants of a Potent, Broad-Spectrum Inhibitor. *Biochemistry 39*, 4288−4298.
(15) Toney, J. H., Hammond, G. G., Fitzgerald, P. M. D., Sharma, N., Balkovec, J. M., Rouen, G. P., Olson, S. H., Hammond, M. L., Greenlee, M. L., and Gao, Y.-D. (2001) Succinic Acids as Potent Inhibitors of Plasmid-borne IMP-1 Metallo-β-lactamase. *J. Biol. Chem. 276*, 31913−31501.
(16) Yamaguchi, Y., Kuroki, T., Yasuzawa, H., Higashi, T., Jin, W., Kawanami, A., Yamagata, Y., Arakawa, Y., Goto, M., and Kurosaki, H. (2005) Probing the role of Asp120(81) of metallo-β-lactamase (IMP-1) by site-directed mutagenesis, kinetic studies, and X-ray crystallography. *J. Biol. Chem. 280*, 20824−20832.
(17) Costello, A., Periyannan, G., Yang, K. W., Crowder, M. W., and Tierney, D. L. (2006) Site-selective binding of Zn(II) to metallo-β-lactamase L1 from *Stenotrophomonas maltophilia*. *J. Biol. Inorg. Chem. 11*, 351−358.
(18) Costello, A. L., Sharma, N. P., Yang, K. W., Crowder, M. W., and Tierney, D. L. (2006) X-ray absorption spectroscopy of the zinc bnding sites in the class B2 metallo-β-lactamase ImiS from *Aeromonas veronii bv. sobria*. *Biochemistry 45*, 13650−13658.
(19) Hawk, M. J., Breece, R. M., Hajdin, C. E., Bender, K. M., Hu, Z., Costello, A. L., Bennett, B., Tierney, D. L., and Crowder, M. W. (2009) Differential binding of Co(II) and Zn(II) to metallo-β-lactamase Bla2 from *Bacillus anthracis*. *J. Am. Chem. Soc. 131*, 10753−10762.
(20) Hu, Z., Periyannan, G., Bennett, B., and Crowder, M. W. (2008) Role of the Zn_1 and Zn_2 sites in metallo-β-lactamase L1. *J. Am. Chem. Soc. 130*, 14207−14216.
(21) Periyannan, G., Costello, A. L., Tierney, D. L., Yang, K. W., Bennett, B., and Crowder, M. W. (2006) Sequential binding of cobalt(II) to metallo-β-lactamase CcrA. *Biochemistry 45*, 1313−1320.
(22) Gonzalez, J. M., Medrano Martin, F. J., Costello, A. L., Tierney, D. L., and Vila, A. J. (2007) The Zn_2 position in metallo-β-lactamases is critical for activity: a study on chimeric metal sites on a conserved protein scaffold. *J. Mol. Biol. 373*, 1141−1156.
(23) Orellano, E. G., Girardini, J. E., Cricco, J. A., Ceccarelli, E. A., and Vila, A. J. (1998) Spectroscopic characterization of a binuclear metal site in *Bacillus cereus* β-lactamase II. *Biochemistry 37*, 10173−10180.
(24) Crowder, M. W., Walsh, T. R., Banovic, L., Pettit, M., and Spencer, J. (1998) Overexpression, Purification, and Characterization of the Cloned Metallo-β-Lactamase L1 from *Stenotrophomonas maltophilia*. *Antimicrob. Agents Chemother. 42*, 921−926.
(25) McManus-Munoz, S., and Crowder, M. W. (1999) Kinetic mechanism of metallo-β-lactamase L1 from *Stenotrophomonas maltophilia*. *Biochemistry 38*, 1547−1553.
(26) Segel, I. H. (1993) *Enzyme Kinetics*, John Wiley and Sons, Inc., New York.
(27) Thomas, P. W., Stone, E. M., Costello, A., Tierney, D. L., and Fast, W. (2005) The quorum-quenching lactonase from *Bacillus thuringiensis* is a metalloprotein. *Biochemistry 44*, 7559−7569.
(28) Newville, M. (2001) IFEFFIT: interactive XAFS analysis and FEFF fitting. *J. Synchrotron Radiat. 8*, 322−324.
(29) Ankudinov, A. L., Ravel, B., Rehr, J. J., and Conradson, S. D. (1998) Real-space multiple-scattering calculation and interpretation of x-ray-absorption near-edge structure. *Phys. Rev. B 58*, 7565−7576.
(30) Laraki, N., Franceschini, N., Rossolini, G. M., Santucci, P., Meunier, C., dePauw, E., Amicosante, G., Frere, J. M., and Galleni, M. (1999) Biochemical Characterization of the *Pseudomonas aeruginosa* 101/1477 Metallo-β-Lactamase IMP-1 Produced by *Escherichia coli*. *Antimicrob. Agents Chemother. 43*, 902−906.
(31) Moali, C., Anne, C., Lamotte-Brasseur, J., Groslambert, S., Devreese, B., Van Beeumen, J., Galleni, M., and Frere, J. M. (2003) Analysis of the importance of the metallo-β-lactamase active site loop in substrate binding and catalysis. *Chem. Biol. 10*, 319−329.
(32) Wang, Z., and Benkovic, S. J. (1998) Purification, Characterization, and Kinetic Studies of Soluble *Bacteroides fragilis* Metallo-β-Lactamase. *J. Biol. Chem. 273*, 22402−22408.
(33) Rasia, R. M., and Vila, A. J. (2003) Mechanistic study of the hydrolysis of nitrocefin mediated by *B. cereus* metallo-β-lactamase. *ARKIVOC 3*, 507−516.
(34) Crowder, M. W., Yang, K. W., Carenbauer, A. L., Periyannan, G., Seifert, M. A., Rude, N. E., and Walsh, T. R. (2001) The Problem of a Solvent Exposable Disulfide when Preparing Co(II)-Substituted Metallo-β-Lactamase L1 from *Stenotrophomonas maltophilia*. *J. Biol. Inorg. Chem. 6*, 91−99.
(35) Garmer, D. R., and Krauss, M. (1993) *Ab Initio* Quantum Chemical Study of the Cobalt d-d Spectroscopy of Several Substituted Zinc Enzymes. *J. Am. Chem. Soc. 115*, 10247−10257.
(36) Bennett, B. (2010) EPR of cobalt-substituted zinc enzymes, in *Metals in Biology - Applications of high-resolution EPR to metalloenzymes* (Hanson, G. R., Ed.) pp 345−370, Springer, Berlin.
(37) Bennett, B., Antholine, W. E., D'Souza, V. M., Chen, G. J., Ustinyuk, L., and Holz, R. C. (2002) Structurally distinct active sites in the copper(II)- substituted aminopeptidases from *Aeromonas proteolytica* and *Escherichia coli*. *J. Am. Chem. Soc. 124*, 13025−13034.
(38) Wright, G. D. (2011) Molecular mechanisms of antibiotic resistance. *Chem. Commun. 47*, 4055−4061.
(39) Walsh, C. T., and Wright, G. D. (2005) Introduction: Antibiotic resistance. *Chem. Rev. 105*, 391−393.
(40) Drawz, S. M., and Bonomo, R. A. (2010) Three decades of β-lactamase inhibitors. *Clin. Microbiol. Rev. 23*, 160−201.

(41) Hammond, G. G., Huber, J. L., Greenlee, M. L., Laub, J. B., Young, K., Silver, L. L., Balkovec, J. M., Pryor, K. D., Wu, J. K., Leiting, B., Pompliano, D. L., and Toney, J. H. (1999) Inhibition of IMP-1 Metallo-β-Lactamase and Sensitization of IMP-1 Producing Bacteria by Thioester Derivatives. *FEMS Microbiol. Lett. 459*, 289−296.

(42) Kurosaki, H., Yamaguchi, Y., Higashi, T., Soga, K., Matsueda, S., Yumoto, H., Misumi, S., Yamagata, Y., Arakawa, Y., and Goto, M. (2005) Irreversible inhibition of metallo-β-lactamase (IMP-1) by 3-(3-mercaptopropionylsulfanyl)-propionic acid pentafluorophenyl ester. *Angew. Chem., Int. Ed. 44*, 3861−3864.

(43) Lassaux, P., Hamel, M., Gulea, M., Delbruck, H., Mercuri, P. S., Horsfall, L., Dehareng, D., Kupper, M., Frere, J. M., Hoffmann, K., Galleni, M., and Bebrone, C. (2010) Mercaptophosphonate compounds as broad-spectrum inhibitors of the metallo-β-lactamases. *J. Med. Chem. 53*, 4862−4876.

(44) Moloughney, J. G., Thomas, J. D., and Toney, J. H. (2005) Novel IMP-1 metallo-β-lactamase inhibitors can reverse Meropenem resistance in *Escherichia coli* expressing IMP-1. *FEMS Microbiol. Lett. 243*, 65−71.

(45) Siemann, S., Brewer, D., Clarke, A. J., Dmitrienko, G. I., Lajoie, G., and Viswanatha, T. (2002) IMP-1 metallo-β-lactamase: effect of chelators and assessment of metal requirement by electrospray mass spectrometry. *Biochim. Biophys. Acta, Gen. Subj. 1571*, 190−200.

(46) Toney, J. H., and Moloughney, J. G. (2004) Metallo-β-lactamase inhibitors: promise for the future? *Curr. Opin. Invest. Drugs 5*, 823−826.

(47) Wang, C., and Guo, H. (2007) Inhibitor binding by metallo-β-lactamase IMP-1 from *Pseudomonas aeruginosa*: Quantum mechanical/molecular mechanical simulations. *J. Phys. Chem. B 111*, 9986−9992.

(48) Garrity, J. D., Bennett, B., and Crowder, M. W. (2005) Direct evidence that reaction intermediate in metallo-β-lactamase is metal bound. *Biochemistry 44*, 1078−1087.

(49) Sharma, N. P., Hajdin, C., Chandrasekar, S., Bennett, B., Yang, K. W., and Crowder, M. W. (2006) Mechanistic studies on the mononuclear Zn(II)-containing metallo-β-lactamase ImiS from *Aeromonas sobria*. *Biochemistry 45*, 10729−10738.

(50) Goto, M., Takahashi, T., Yamashita, F., Koreeda, A., Mori, H., Ohta, M., and Arakawa, Y. (1997) Inhibition of the Metallo-b-Lactamase Produced from *Serratia marcescens* by Thiol Compounds. *Biol. Pharm. Bull. 20*, 1136−1140.

(51) Materon, I. C., and Palzkill, T. (2001) Identification of residues critical for metallo-β-lactamase function by codon randomization and selection. *Protein Sci. 10*, 2556−2565.

(52) Oelschlaeger, P., Mayo, S. L., and Pleiss, J. (2005) Impact of remote mutations on metallo-β-lactamase substrate specificity: implications for the evolution of antibiotic resistance. *Protein Sci. 14*, 765−774.

(53) Bounaga, S., Laws, A. P., Galleni, M., and Page, M. I. (1998) The Mechanism of Catalysis and the Inhibition of the *Bacillus cereus* Zinc-Dependent β-Lactamase. *Biochem. J. 331*, 703−711.

(54) Wang, Z., Fast, W., and Benkovic, S. J. (1998) Direct Observation of an Enzyme-Bound Intermediate in the Catalytic Cycle of the Metallo-β-Lactamase from *Bacteroides fragilis*. *J. Am. Chem. Soc. 120*, 10788.

(55) Carfi, A., Duee, E., Galleni, M., Frere, J. M., and Dideberg, O. (1998) 1.85 A Resolution Structure of the ZincII β-Lactamase II from *Bacillus cereus*. *Acta Crystallogr. D54*, 313−323.

(56) Gonzales, J. M., Buschiazzo, A., and Vila, A. J. (2010) Evidence of Adaptability in metal coordination geometry and active-site loop conformation among B1 metallo-β-lactamases. *Biochemistry 49*, 7930−7938.

(57) Gardonio, D., and Siemann, S. (2009) Chelator-facilitated chemical modification of IMP-1 metallo-β-lactamase and its consequences on metal binding. *Biochem. Biophys. Res. Commun. 381*, 107−111.

(58) Wommer, S., Rival, S., Heinz, U., Galleni, M., Frere, J. M., Franceschini, N., Amicosante, G., Rasmussen, B., Bauer, R., and Adolph, H. W. (2002) Substrate-activated zinc binding of metallo-β-lactamases - Physiological importance of the mononuclear enzymes. *J. Biol. Chem. 277*, 24142−24147.

(59) Heinz, U., and Adolph, H. W. (2004) Metallo-β-lactamases: two binding sites for one catalytic metal ion? *Cell. Mol. Life Sci. 61*, 2827−2839.

(60) Fast, W., Wang, Z., and Benkovic, S. J. (2001) Familial Mutations and Zinc Stoichiometry Determine the Rate-Limiting Step of Nitrocefin Hydrolysis by Metallo-β-Lactamase from *Bacteroides fragilis*. *Biochemistry 40*, 1640−1650.

(61) Paul-Soto, R., Hernandez-Valladares, M., Galleni, M., Bauer, R., Zeppezauer, M., Frere, J. M., and Adolph, H. W. (1998) Mono- and Binuclear Zn-β-Lactamase from *Bacteroides fragilis*: Catalytic and Structural Roles of the Zinc Ions. *FEBS Lett. 438*, 137−140.

(62) Dal Peraro, M., Vila, A. J., and Carloni, P. (2004) Substrate binding to Mononuclear metallo-β-lactamase from *Bacillus cereus*. *Proteins: Struct., Funct., Bioinf. 54*, 412−423.

(63) de Seny, D., Heinz, U., Wommer, S., Kiefer, M., Meyer-Klaucke, W., Galleni, M., Frere, J. M., Bauer, R., and Adolph, H. W. (2001) Metal ion binding and coordination geometry for wild type and mutants of metallo-β-lactamase from *Bacillus cereus* 569/H/9 (BcII) - A combined thermodynamic, kinetic, and spectroscopic approach. *J. Biol. Chem. 276*, 45065−45078.

(64) Estiu, G. L., Rasia, R. M., Cricco, J. A., Vila, A. J., and Zerner, M. C. (2002) Is there a bridging ligand in metal-substituted zinc β-lactamases? A spectroscopic and theoretical answer. *Int. J. Quantum Chem. 88*, 118−132.

(65) Paul-Soto, R., Bauer, R., Frere, J. M., Galleni, M., Meyer-Klaucke, W., Nolting, H., Rossolini, G. M., de Seny, D., Hernandez-Villadares, M., Zeppezauer, M., and Adolph, H. W. (1999) Mono- and Binuclear Zn2+ β-Lactamase. *J. Biol. Chem. 274*, 13242−13249.

(66) Rasia, R. M., and Vila, A. J. (2002) Exploring the role and the binding affinity of a second zinc equivalent in B. cereus metallo-β-lactamase. *Biochemistry 41*, 1853−1860.

(67) Selevsek, N., Rival, S., Tholey, A., Heinzle, E., Heinz, U., Hemmingsen, L., and Adolph, H. W. (2009) Zinc ion-induced domain organization in metallo-β-lactamases. A flexible "zinc arm" for rapid metal ion transfer. *J. Biol. Chem. 284*, 16419−16431.

(68) Jacquin, O., Balbeur, D., Damblon, C., Marchot, P., dePauw, E., Roberts, G. C. K., Frere, J. M., and Matagne, A. (2009) Positively cooperative binding of zinc ions to *Bacillus cereus* 569/H/9 β-lactamase II suggests that the binuclear enzyme is the only relevant form for catalysis. *J. Mol. Biol. 392*, 1278−1291.

(69) Badarau, A., Damblon, C., and Page, M. I. (2007) The activity of the dinuclear cobalt-β-lactamase from *Bacillus cereus* in catalysing the hydrolysis of β-lactams. *Biochem. J. 401*, 197−203.

(70) Badarau, A., and Page, M. I. (2006) Enzyme deactivation due to metal ion dissociation during turnover of the cobalt-β-lactamase catalyzed hydrolysis of β-lactams. *Biochemistry 45*, 11012−11020.

(71) Badarau, A., and Page, M. I. (2008) Loss of enzyme activity during turnover of the Bacillus cereus β-lactamase catalysed hydrolysis of β-lactams due to loss of zinc ions. *J. Biol. Inorg. Chem. 13*, 919−928.

(72) Llarrull, L. I., Tioni, M. F., Kowalski, J., Bennett, B., and Vila, A. J. (2007) Evidence for a Dinuclear Active Site in the Metallo-β-lactamase BcII with Substoichiometric Co(II): A new model for metal uptake. *J. Biol. Chem. 282*, 30586−30595.